

# Quasi-one and two-dimensional transitions of gases adsorbed on nanotube bundles

S. M. Gatica<sup>1</sup>, M. J. Bojan<sup>2</sup>, G. Stan<sup>3</sup>, and M. W. Cole<sup>4</sup>

<sup>1</sup> *Departamento de Física, Facultad de Ciencias Exactas y Naturales, Universidad de Buenos Aires, 1428, Buenos Aires, Argentina.*

<sup>2</sup> *Departments of Chemistry Pennsylvania State University University Park, PA 16802, USA*

<sup>3</sup> *Institute for Physical Science and Technology and Department of Chemical Engineering, University of Maryland, College Park, MD 20742, USA.*

<sup>4</sup> *Departments of Physics, Pennsylvania State University University Park, PA 16802, USA*  
(October 31, 2018)

## Abstract

Grand canonical Monte Carlo simulations have been performed to determine the adsorption behavior of Ar and Kr atoms on the exterior surface of a rope (bundle) consisting of many carbon nanotubes. The computed adsorption isotherms reveal phase transitions associated with the successive creation of quasi-one dimensional lines of atoms near and parallel to the intersection of two adjacent nanotubes.

## I. INTRODUCTION

Much attention has focused recently on the problem of gas adsorption within bundles (“ropes”) of carbon nanotubes [1–13]. For small atoms and molecules, both the cylindrical spaces within individual tubes and the interstitial channels between tubes are regions of very attractive potential energy for adsorption. Larger molecules experience a similar attraction within the tubes (but not within the interstitial region, unless swelling occurs). In either case, there occurs significant uptake, within these respective regions, at pressures  $P$  below saturated vapor pressure  $P_0$  (svp). It was noted recently by Williams and Eklund [9] that finite bundles of carbon nanotubes ought to exhibit additional, significant adsorption on the external surface of the bundles. In the thermodynamic limit of an infinite array, such external adsorption represents a negligible fraction of the total. Typical finite bundles, however, have radius  $R \sim 100$  Å and are expected to manifest significant external adsorption. Indeed, experiments of Talapatra *et al.* [14] have been interpreted as providing evidence of such external adsorption in the case of  $\text{CH}_4$  molecules, Ne and Xe atoms.

In this paper we formulate a simple model of this system with which we explore the phenomenon of external adsorption. We suppose that the nanotube bundle of Fig. 1 is our subject of investigation. This assumption provides us with a normalization factor (essentially a surface/volume ratio) required for a specific prediction of the adsorbate mass per mass of substrate (and nothing more). Any alternative geometry requires a “renormalization”

factor, discussed below. Our actual calculations of external adsorption are performed with a simplified abstraction of figure 1. Specifically, the model employs a periodic, planar array of parallel cylinders representing the nanotubes. This planar model should be an adequate approximation to the real situation (tubes at the perimeter of a rope) in an experimental situation for which  $R$  greatly exceeds the radius ( $\sim 7 \text{ \AA}$ ) of an individual tube. Our method of evaluating the adsorption is computer simulation, using the grand canonical Monte Carlo (GCMC) method. With this well developed technique we are able to demonstrate the existence of several phase transitions in the film. These include both two-dimensional (2D) transitions (analogous to layering transitions on flat surfaces) and quasi-1D transitions (analogous to ones on similar quasi-1D geometries, such as a surface facet cut close to that of a low index surface). [15]

The outline of this paper is the following. The following section describes our model potential and computational method. Section III describes our results. In section IV, we describe implications for experiments studying such systems.

## II. METHOD

As in most adsorption studies on graphite or carbon nanotubes, the adsorption potential assumed here is a pairwise sum of two-body interactions  $U(\mathbf{x})$  between a molecule and the nanotube's carbon atoms [16,17]:

$$V(\mathbf{r}) = \sum_i U(\mathbf{r} - \mathbf{R}_i) \quad (1)$$

where  $\mathbf{r}$  is the position of the molecule and  $\mathbf{R}_i$  is the position of a C atom. The pair potential is assumed to be isotropic and of Lennard-Jones form:  $U(r) = 4\epsilon[(\sigma/r)^{12} - (\sigma/r)^6]$ . Although we neglect here the effect of anisotropy for adsorption on graphite [18], the potential considered is suitable for our qualitative study. The LJ parameters for the Ar-C and Kr-C interaction are obtained with semiempirical combining rules from the corresponding LJ parameters : [19–22]:

$$\begin{aligned} \sigma_{gC} &= \frac{\sigma_{gg} + \sigma_{CC}}{2} \\ \epsilon_{gC} &= \sqrt{\epsilon_{gg} \epsilon_{CC}} \end{aligned} \quad (2)$$

The parameter values used in this study are listed in the Table I.

Another simplifying assumption employed here is the replacement of discrete carbon atoms by a continuous cylindrical sheet of matter; this should not drastically affect the adsorbate's behavior except when the adjacent tubes are in perfect registry, an unlikely situation. The resulting potential at distance  $r$  from the nanotube axis, outside of the tube, is [24]:

$$V(r; R) = 3 \pi \theta \epsilon \sigma R \left[ \frac{21}{32} \left( \frac{\sigma}{r} \right)^{11} M_{11}(x) - \left( \frac{\sigma}{r} \right)^5 M_5(x) \right] \quad (3)$$

where  $\theta = 0.38 \text{ \AA}^2$  is the surface density of C atoms and  $R$  is the radius of the nanotube. We use the integrals

$$M_n(x) = \int_0^\pi d\varphi \frac{1}{(1 + x^2 - 2x\cos\varphi)^{n/2}}. \quad (4)$$

Finally, the adsorption potential on the external surface of the nanotube bundle is obtained by summing up the interactions of the molecule with all the nanotubes in the bundle.

We perform GCMC simulations of Ar and Kr interacting with the outer wall of a bundle of (10,10) tubes lined up to create a “flat” surface with grooves. In the GCMC simulations, the chemical potential, temperature and volume are held constant while the number of particles varies. This technique is standard and has been described in textbooks [25,26], so only the details will be given here. Three kinds of moves are performed: displacement of a molecule, creation of a particle and deletion of a particle. In the original method of Norman and Filinov, [27] these moves were done in equal proportion (33% each). In our simulations however, the percentage of attempted creation and deletions was set at 40% each while 20% of the attempted moves were displacements. This was done because the acceptance rate for displacement moves was typically much higher than the acceptance rates for the creation/deletion moves. By increasing the percentage of attempts, the total number of creations and deletions that are accepted is increased, thus reducing the computation time somewhat. It is still necessary to perform an increased number of moves in the transition regions and in the high density regions to insure good thermodynamic averages. For a single isotherm point typically,  $3 \times 10^6$  moves were performed to equilibrate the system and  $10^6$  moves were used for data gathering.

The Ar-Ar and Kr-Kr pair interactions were taken as a 12-6 Lennard-Jones potential. In representing the interaction of the gas with the bundle of nanotubes, only one tube was modeled, with the groove in the center of the simulation cell and the apex of the tube at the periodically replicated boundary. Since the distance between the axis of two neighboring nanotubes is 17 Å, one of the cell boundaries (the x direction) was fixed at this length. The tube length (y-dimension) was set at  $10\sigma_{gg}$  and periodic boundary conditions were used in these two dimensions. The height of the simulation box (z-direction) was set at 40 Å where a reflecting surface was used. Figure 2 depicts the adsorption potential for the case of an Ar atom in the unit cell.

In Table II we compare values of the well depth found here with those found for Ne, Ar and Kr atoms in related geometries: the interstitial channel, inside the nanotubes and on the surface of graphite. It is seen that Ne experiences its most attractive potential in the interstitial channels, while the other (larger) atoms find the external groove to be most attractive. In the latter cases, the well is nearly twice as attractive as the well on the graphite surface. This can be understood from the fact that the most favorable position in the groove case corresponds to the optimal distance from each of the contributing tubes and each tube contributes a well depth equal to 85% of that on planar graphite, so that the groove is 70% more attractive than graphite. This situation is similar to recent measurements by Talapatra *et al.* [14]. Their reported binding energies for Ne, Xe and CH<sub>4</sub> adsorbed in closed-ended nanotubes are about 75% larger than on planar graphite.

Simulations of Ar interacting with the bundle surface at temperatures ranging from 30K to 68K were performed. The effect of molecular size was tested by varying the size ( $\sigma$ ) of Argon (ranging from 3.6 to 4.0 Å) without varying the interaction strength. These results will be referred to as “artificial Argon”. Also, simulations of the adsorption of Kr on this surface for temperatures ranging from T = 57K to 97K were performed to look at the effect

of increased interaction strength.

### III. RESULTS

Fig. 3 presents results for the adsorption of Ar at low temperature (less than or of order one-half of the  $\epsilon_{ArAr}$  parameter). None of these results exhibits any evidence of hysteresis. The coverage in this and subsequent figures is expressed in two alternative forms on the ordinate scales. On the left appears a number equal to the number of atoms per unit length of the simulation cell, which is  $10\sigma_{ArAr}=34 \text{ \AA}$ . For a single line of atoms at close packing, this corresponds to about nine atoms per 1d chain. Our checks show that the simulation results do not differ significantly if we increase this periodicity length. The right scale expresses the coverage in adsorbate moles per gram of carbon. That calculation is carried out by assuming the geometry to be the hexagonal structure of Fig. 1 (which contains  $N_t=37$  nanotubes and  $N_g=18$  grooves on its perimeter). If the bundle size or shape is different, one merely corrects the axis label by multiplying the right scale's values by a factor  $(37 N_g)/(18 N_t)$ .

One observes in Fig. 3 that the isotherm at  $T=30 \text{ K}$  consists of a series of plateaus, separated by steps. Each plateau represents a region of stability (over a range of  $P$ ) of a particular structure, which one observes in the density plots shown in Fig. 4. This behavior is analogous to the stepped isotherms seen in adsorption on flat surfaces, a manifestation of layering transitions on microscopically flat surfaces.

At very low  $P$ , significant adsorption occurs only in a “groove” formed along the contact line of two nanotubes. Below the first plateau, this isotherm coincides with that  $\mu_{1d}(P,T)$  predicted for a purely one-dimensional system, with an additive constant  $V_1$  due to the potential provided by neighboring nanotubes and a small, slowly varying term  $\delta\mu_T$  arising from adatom motion transverse to the groove:

$$\mu = V_1 + \mu_{1d}(P, T) + \delta\mu_T \quad (5)$$

$$\beta \delta\mu_T = \ln[\lambda^2/(\pi \langle r^2 \rangle)]. \quad (6)$$

Here  $1/\beta = k_B T$  and  $\langle r^2 \rangle = 2/(\beta k)$  is the mean square displacement perpendicular to the channel, expressed in terms of the transverse force constant  $k$ , and  $\lambda = \sqrt{(2\pi\beta\hbar^2)/m}$  is the de Broglie thermal wavelength. The values of  $V_1$  and other potential energies at locations of specific 1d lines of atoms are presented in Table III.

Above the plateau associated with saturation (complete filling) of the groove, there occurs a coverage jump near  $P = 10^{-14} \text{ atm.}$  (at  $T=30\text{K}$ ). This corresponds to the appearance of a well-defined “three-channel” regime, the density of which appears in Fig. 4a. Upon further increasing the pressure by a factor of  $\sim 10$ , the coverage jumps by a factor of two, to a regime in which the surface is covered by a striped monolayer film, seen in Fig. 4b. A further increase in  $P$  by a factor of 3,000 results in a transition to a bilayer film, depicted in Fig. 4c. This film grows continuously thereafter, since this is a strongly wetting situation.

The pressures at which these jumps occur can be predicted rather accurately with simple model estimates. For example, the threshold at  $T=30 \text{ K}$  for forming the three-channel state is estimated to be:

$$\mu_3 = V_3 - 4\epsilon_{Ar} + \delta\mu_T = -1352K \quad (7)$$

The factor of four is based on an assumed 4-fold coordination in the “new” pair of channels (beyond the original one), plus an external field  $V_3$  contributed by atoms in the original channel of adatoms. The preceding estimate is close to the value found in the simulation ( $\mu_3 = -1270$  K) for the onset of the three-channel state. Encouraged by this degree of consistency, we estimate the chemical potential threshold for the monolayer, for which there are six channels present:

$$\mu_6 = -3\epsilon_{Ar} + V_6 = -1155K \quad (8)$$

Here the factor of three is derived from one-half of the 6-fold coordination. This numerical result is close to that found in the simulation (near  $P = 10^{-13}$  atm,  $\mu_6 = -1040$  K).

In Fig. 5 we present the adsorption isotherms for Kr at temperatures ranging from 43K to 97K. In the isotherm at  $T=43$ K we find the same transitions than for Ar at 30K. (Notice that the reduced temperatures are the same, i.e.  $43K/\epsilon_{KrKr}=30K/\epsilon_{ArAr} = 0.25$ )

One of the interesting features of these isotherms is the role played by size commensuration in determining the monolayer transition on this surface comprised of nanotubes. This effect is analogous to the role played by the molecular diameter in determining the presence, or absence, of epitaxial phases in monolayer phases on planar surfaces. [28,29] Figure 6 presents isotherms obtained for a set of “artificial Argon” systems; these gases differ from one another in the values of the  $\sigma$  parameter, as indicated. As a result of this variation, the monolayer transition is seen to change in a discontinuous way. For small values of  $\sigma$ , the monolayer consists of 6 lines of atoms. Above a threshold value,  $\sigma=3.8\text{\AA}$ , the monolayer consists of only 5 lines of atoms. This behavior is an expected steric effect. It is interesting to see that there exists a transitional value,  $\sigma \sim 3.6\text{\AA}$ , for which ambiguity is present in the isotherm at this monolayer transition (near  $P=10^{-9}$  atm).

The isotherms for Ar and Kr presented earlier both correspond to the small atom case and therefore we find that the monolayer film consists of six parallel lines of atoms. On the basis of the artificial systems reported in Fig. 6, we expect the monolayer of Xe (not studied here) to correspond to five parallel lines.

#### IV. DISCUSSION

These calculations predict the existence of transitions between unusual phases of matter. The first transition (as a function of  $P$ ) is that between a one-dimensional fluid within a groove and a set of three parallel lines of fluid. Subsequent transitions occur to a monolayer and bilayer phase. Such transitions are possible due to the interaction between one group (e.g., three lines) of particles and other groups which are present in the system, which is taken to be periodic. The observation that a doubling of the transverse cell dimension does not affect the results significantly suggests that these results are present in the infinite system (as is the case in our recent study of the interstitial phase’s condensation transition [12]). Of course, one recognizes that the actual system under investigation is not infinite; it is a quasi-cylindrical bundle of (approximately parallel) nanotubes which is quite finite in transverse dimension. Hence one expects a rounding of the vertical jumps shown here. The degree of rounding depends on the deviation from our assumptions. Once that is known, more realistic simulations can be carried out.

This research has been supported by the National Science Foundation's Focussed Research Group program. We are grateful to Moses Chan, Peter Eklund, John Lewis, Paul Sokol, Bill Steele and Keith Williams for stimulating discussion.

# TABLES

TABLE I. Parameters of the LJ interaction for Ar and Kr. [20,23]

Gas	$\epsilon_{gg}(\text{K})$	$\sigma_{gg}(\text{\AA})$	$\epsilon_{gC}(\text{K})$	$\sigma_{gC}(\text{\AA})$
Ar	120	3.4	57.9	3.4
Kr	171	3.6	69.2	3.5

TABLE II. Characteristic well depths of Ar Kr and Ne in the external surface (ext), the interstitial channel (IC), inside the nanotubes (NT) and on flat graphite (gr). [13]

Gas	$V_{min}^{ext}$ (K)	$V_{min}^{IC}$ (K)	$V_{min}^{NT}$ (K)	$V_{min}^{gr}$ (K)
Ar	-1607	6	-1426	-965
Kr	-2025	2048	-1836	-1220
Ne	-725	-1018	-600	-431



TABLE III. Potential energies of Ar atoms located in the central channel (1) and the following channels numbered from the center to the right (see fig. 4b).

channel	1	2	3	4
V(K)	-1607	-872	-799	-795

## REFERENCES

- [1] V. V. Simonyan, P. Diep, and J. K. Johnson, J. Chem. Phys., **111**, 9778 (1999); Q. Wang and J. K. Johnson, J. Phys. Chem. B **103**, 4809 (1999); Q. Wang, S.R. Challa, D.S. Sholl, and J.K. Johnson, Phys. Rev. Lett. **82**, 956 (1999).
- [2] S. Inoue, N. Ichikuni, T. Suzuki, T. Uematsu, and K. Kaneko, J. Phys. Chem. B **102**, 4689 (1998).
- [3] G. Gao, T. Cagin, and W. A. Goddard III, Phys. Rev. Lett. **80**, 5556 (1998).
- [4] W. Teizer, R. B. Hallock, E. Dujardin, and T. W. Ebbesen, Phys. Rev. Lett. **82**, 5305 (1999) and **84**, 1844 (2000) (*erratum*).
- [5] S. E. Weber, S. Talapatra, C. Journet, A. Z. Zambano and A. D. Migone, Phys. Rev. B **61**, 13150 (2000).
- [6] A. J. Zambano, S. Talapatra and A. D. Migone, "Binding energy and monolayer capacity of Xe on SWNT bundles", submitted to Phys. Rev. 4/00.
- [7] . Y. F. Yin, Tim Mays, and Brian McEnaney, Langmuir **15**, 8714 (1999).
- [8] A. Kuznetsova, J. T. Yates, Jr., J. Liu, and R. E. Smalley, J. Chem. Phys. **112**, 9590 (2000).
- [9] K.A.Williams and P. C. Eklund, Chem. Phys. Lett. **320**, 352 (2000).
- [10] M. S. Dresselhaus, K. A. Williams and P. C. Eklund, MRS Bulletin, **24**, 45 (1999).
- [11] G. Stan and M. W. Cole, J. Low Temp. Phys. **110**, 539 (1998).
- [12] M. W. Cole, V. H. Crespi, G. Stan, C. Ebner, J. M. Hartman, S. Moroni, and M. Boninsegni, Phys. Rev. Lett. **84**, 3883 (2000).
- [13] G. Stan, M. J. Bojan, S. Curtarolo, S. M. Gatica and M. W. Cole, Phys. Rev. B **62**, 2173 (2000).
- [14] S. Talapatra, A.Z. Zambano, S.E. Weber and A.D. Migone, Phys. Rev. Lett. **85**, 138 (2000).
- [15] S. J. Stranick, M. M. Kamna, and P. S. Weiss, Science **266**, 99 (1994).
- [16] The empirical pair potential must be regarded as an effective pair potential. Many-body interactions have been found to yield a  $\sim 15\%$  correction to *em ab initio* pair potential sums, see H.-Y. Kim and M. W. Cole, Phys. Rev. B **35**, 3990 (1987).
- [17] Subsequent to completing the present calculations, we found that three-body interactions (involving the carbon) reduce the well depth of the interaction between atoms within the groove by about 25 per cent. ( M. K. Kostov, J. C. Lewis and M. W. Cole, cond-mat/0007034).
- [18] W. E. Carlos and M. W. Cole, Surf. Sci. **91**, 339 (1980); L. W. Bruch, in *Phase Transitions in Surface Films 2*, H. Taub, G. Torzo, H. J. Lauter, and S. C. Fain, Jr., Eds., pp. 67-82 (Plenum, New York, 1991).
- [19] W. A. Steele, Chem. Rev. **93**, 2355 (1993).
- [20] W. A. Steele, Surf. Sci. **36**, 317 (1973).
- [21] G. Scoles, Intl. J. Quant. Chem. **24**, 475 (1990).
- [22] G. Ihm, M. W. Cole, F. Toigo, and J. R. Klein, Phys. Rev. A **42**, 5244 (1990).
- [23] R. O. Watts and I. J. McGee, *Liquid State Chemical Physics* (Wiley, New York, 1976).
- [24] G. Stan and M. W. Cole, Surf. Sci. **395**, 280 (1998).
- [25] D. Frenkel and B. Smit, Understanding Molecular Simulation, (Academic Press, 1996).
- [26] M.P. Allen and D.J Tildesley, Computer Simulations of Liquids (Clarendon Press, Oxford, 1987).

- [27] G.E. Norman and V.V. Filinov, High Temp. (USSR) **7**, 216 (1969).
- [28] L. M. Sander and J. Hautman, Phys. Rev. B **29**, 2171 (1984).
- [29] L. W. Bruch, M. W. Cole and E. Zaremba, Physical Adsorption (Oxford U. P.,1997), Chapter 5.

## FIGURES

FIG. 1. A model nanotube bundle possessing 37 tubes and 18 external grooves.

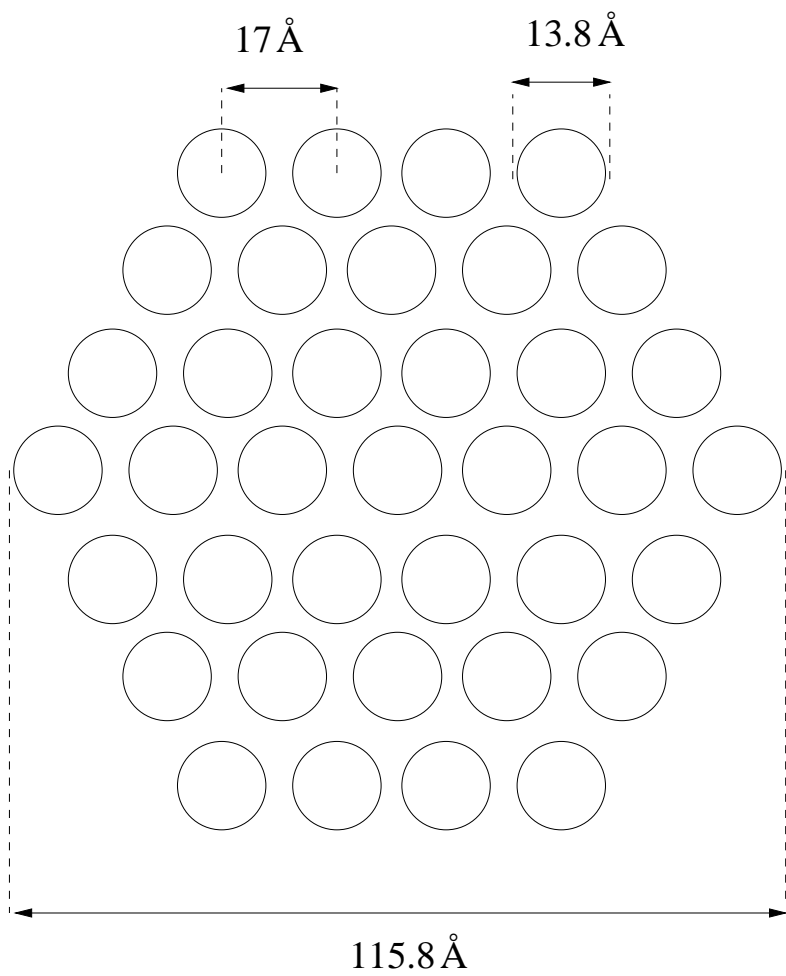
FIG. 2. Depiction of one unit cell of the one-dimensionally periodic line of nanotubes assumed in the simulations. The contours correspond to constant potential energy values  $V/\epsilon_{ArC} = -25, -20, -15, -10, -5, -1$  from darker to lighter. The dashed lines correspond to the cylindrical nanotube surface.

FIG. 3. Adsorption isotherms for Ar at various temperatures, indicated by the symbols in the figure. The left ordinate label  $\langle N \rangle$  is defined in text. The right scale, as described in text, assumes a bundle having the structure depicted in figure 1.

FIG. 4. Density of Ar atoms as a function of the coordinates perpendicular to the axis of the bundle. The temperature is 30K and the pressure is a)  $P=0.36 \cdot 10^{-13} \text{atm}$  ( $\langle N \rangle=27.3$ ), b)  $P=0.4 \cdot 10^{-12} \text{atm}$  ( $\langle N \rangle=54.0$ ), c)  $P=0.59 \cdot 10^{-9} \text{atm}$  ( $\langle N \rangle=99.5$ ). The contours show constant density values of  $2 \text{\AA}^{-2}$  (thick) and  $0.2 \text{\AA}^{-2}$  (thin).

FIG. 5. Adsorption isotherms for Kr at several temperatures indicated in the legend.

FIG. 6. Adsorption isotherms for four gases having  $\epsilon_{gg} = \epsilon_{ArAr}$  and  $\sigma_{gg}$  indicated in the inbox. The temperature is 40K.



**FIG. 1**

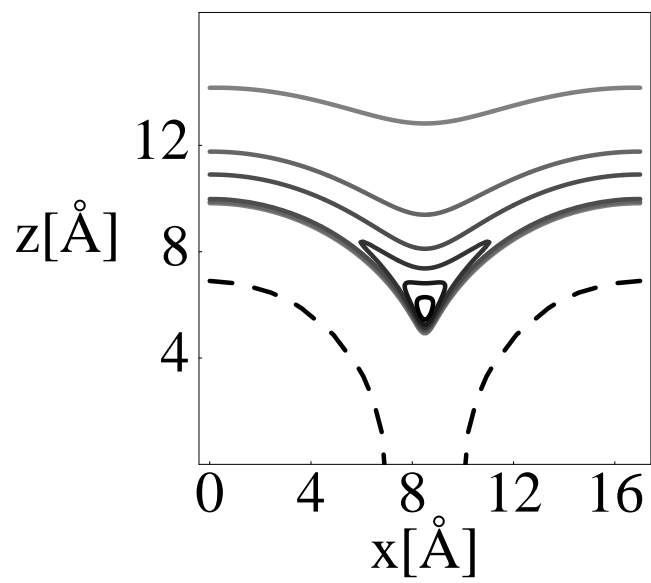


FIG. 2

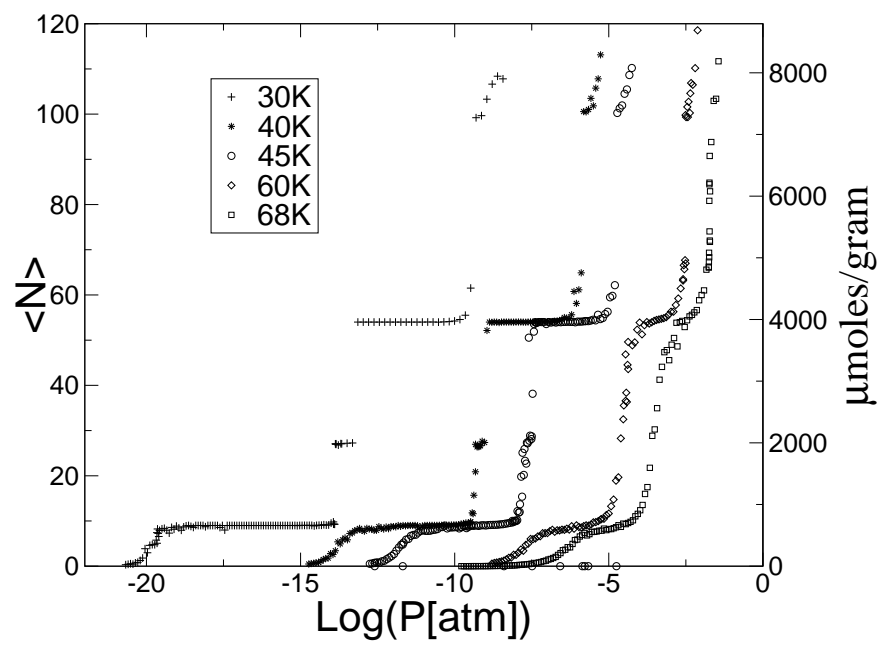


FIG. 3

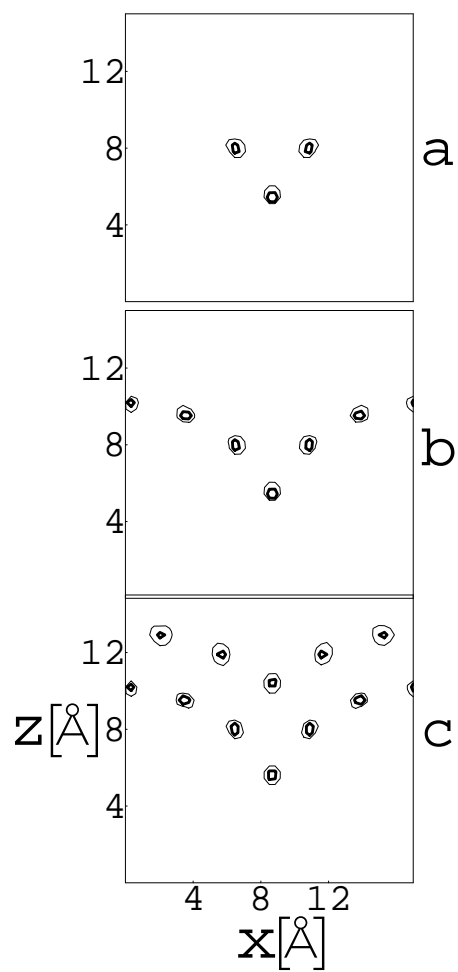


FIG. 4



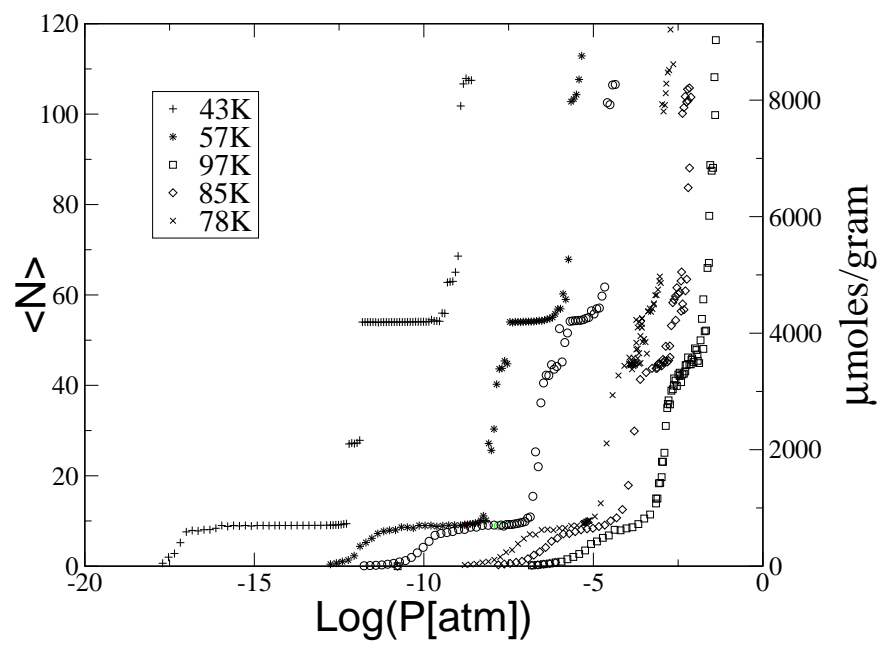


FIG. 5

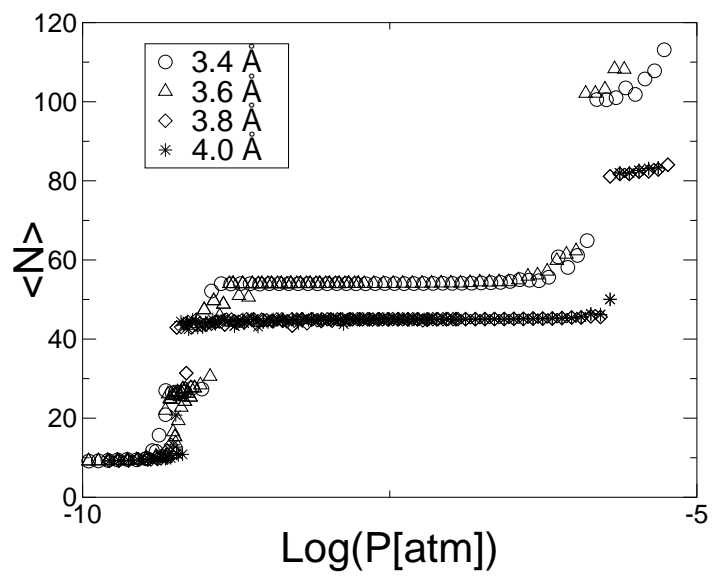


FIG. 6